NIH Public Access
Author Manuscript

Circ Cardiovasc Imaging. Author manuscript; available in PMC 2011 March 25.

Iodinated Contrast Opacification Gradients in Normal Coronary Arteries Imaged with Prospectively ECG-Gated Single Heart Beat 320-Detector Row Computed Tomography

Michael L. Steigner, M.D., **Dimitrios Mitsouras, Ph.D.**, **Amanda G. Whitmore, B.A.**, **Hansel J. Otero, M.D.**, **Chunliang Wang, M.D.**[1], **Orla Buckley, M.D.**, **Noah A. Levit, B.S.**, **Alia Z. Hussain, M.D.**, **Tianxi Cai, Ph.D.**[2], **Richard T. Mather, Ph.D.**[4], **Örjan Smedby, M.D.**[3], **Marcelo F. DiCarli, M.D.**, and **Frank J. Rybicki, M.D.,Ph.D.**

[1] Chunliang Wang, M.D., Dept of Radiology (IMH), Linköping University, Linköping, Sweden; Center for Medical Image Science and Visualization (CMIV), Linköping University, Linköping, Sweden

[2] Tianxi Cai, Ph.D Department of Biostatistics, Harvard School of Public Health, Boston, MA, USA

[3] Örjan Smedby, M.D., Dr. Med. Sci., Dept of Radiology (IMH), Linköping University, Linköping, Sweden; Center for Medical Image Science and Visualization (CMIV), Linköping University, Linköping, Sweden

[4] Richard T. Mather, Ph.D, Toshiba America Medical Systems, Tustin, CA, USA

Abstract

Background—To define and evaluate coronary contrast opacification gradients using prospectively ECG-gated single heart beat 320-detector row coronary angiography (CTA).

Methods and Results—Thirty-six patients with normal coronary arteries determined by 320×0.5 mm detector row coronary CTA were retrospectively evaluated with customized image post-processing software to measure Hounsfield Units (HU) at 1 mm intervals orthogonal to the artery center line. Linear regression determined correlation between mean HU and distance from the coronary ostium (regression slope defined as the distance gradient G_d), lumen cross-sectional area (G_a), and lumen short axis diameter (G_s). For each gradient, differences between the three coronary arteries were analyzed with ANOVA. Linear regression determined correlations between measured gradients, heart rate, body-mass index (BMI), and cardiac phase. To determine feasibility in lesions, all three gradients were evaluated in 22 consecutive patients with left anterior descending artery lesions greater than or equal to 50% stenosis. For all 3 coronary arteries in all patients, the gradients G_a and G_s were significantly different from zero ($p<0.0001$), highly linear (Pearson r values 0.77-0.84), and had no significant difference between the LAD, LCx, and RCA ($p>0.503$). The distance gradient G_d demonstrated nonlinearities in a small number of vessels and was significantly smaller in the RCA when compared to the left coronary system ($p<0.001$). Gradient variations between cardiac phases, heart rates, BMI, and readers were low. Gradients in patients with lesions were significantly different ($p<0.021$) than in patients considered normal by CTA.

Corresponding author: Frank J. Rybicki, MD, PhD, Applied Imaging Science Laboratory, Department of Radiology, Noninvasive Cardiovascular Imaging Program, Brigham and Women's Hospital and Harvard Medical School, 75 Francis Street, Boston, MA 02115, Tel: 617 732 7206, Fax: 617 264 5245, frybicki@partners.org.

Conclusions—Measurement of contrast opacification gradients from temporally uniform coronary CTA demonstrates feasibility and reproducibility in patients with normal coronary arteries. For all patients the gradients defined with respect to the coronary lumen cross-sectional area and short axis diameters are highly linear, not significantly influenced by the coronary artery (LAD vs LCx vs RCA), and have only small variation with respect to patient parameters. Preliminary evaluation of gradients across coronary artery lesions is promising but requires additional study.

Keywords

computed tomography; coronary vessels; imaging

Introduction

The number and width of CT detector rows determine the craniocaudal coverage per gantry rotation. Coronary CT angiography (CTA) with 64 detector rows, each 0.5 mm wide, simultaneously records 32 mm (64×0.5 mm) of image data per gantry rotation. Thus, multiple gantry rotations are combined for image interpretation; each rotation contributes a cardiac subvolume. Spatial misalignment between subvolumes is termed stair-step or slab artifact. Temporal misalignment between subvolumes for coronary contrast opacification refers to differences in attenuation induced by time differences between acquisitions of the superior versus inferior subvolumes.

Wide area detector CT provides up to 160 mm (320×0.5 mm detector rows) craniocaudal coverage, eliminating spatial and temporal misalignment in coronary CTA. Whole volume acquisition enables quantification of the spatial variation in Hounsfield Units (HU) over the entire coronary at a single point in time. We define the term "coronary contrast opacification gradient" to describe these changes. If these parameters could be rapidly and reproducibly computed, they would have the potential to extend the role of cardiac CT beyond coronary artery morphology alone. One advantage could be realized in patients with diffuse coronary artery disease (CAD) where the lumen area is diffusely smaller than normal [1,2] and thus there is no normal reference segment for quantitative measures. Moreover, lesions with less than 50% narrowing in these patients are considered a substrate for plaque rupture and acute coronary syndrome. [3-5]

An initial experiment of normal coronary arteries imaged by CT in a single R-R measured the difference of the mean HU between the ostium and the point where the normal vessel tapered to 2.5 mm diameter. This work showed a small but consistent decrease in contrast opacification from the proximal to distal coronary artery. [6]

This project extends the quantitative assessment of normal coronary contrast attenuation by sampling coronary HU every 1 mm along the artery. This high rate of sampling enables evaluation of opacification gradients as opposed to difference measurements. Although coronary segmentation is available for several post-processing software packages, customized software is required to extract the mean HU orthogonal to the center line at 1 mm intervals. Using a customized software package developed for coronary contrast opacification gradients, the primary purpose of this study was to demonstrate that three opacification gradients can be noninvasively measured using single heart beat 320-detector row CT in patients with normal arteries. The first gradient, the "distance gradient" (denoted G_d), is defined as the change in HU per cm of coronary artery. The second and third gradients are defined as the change in HU with respect to the coronary artery lumen area (G_a) and short axis diameter (G_s) orthogonal to the center line, respectively. The second purpose of this study was to evaluate the properties of the three gradients, including

goodness-of-fit of the respective linear model, potential differences between the three main coronary arteries, and the influence of patient heart rate and body mass index.

Materials and Methods

Patients

The institutional human research committee approved this retrospective study and waived the need for written informed consent. All patients had clinical indications for coronary CTA. We retrospectively evaluated 36 consecutive single R-R 320 × 0.5 mm detector configuration (Toshiba AquilionOne Dynamic Volume CT, Tochigi-ken, Japan) prospectively ECG-gated coronary CTA patients with normal coronary arteries (Table 1). The diagnosis of normal coronary arteries was obtained from the CT imaging reports at our institution. The phase window included 25% (60-85%) of the R-R interval; this protocol has an estimated radiation dose of 5-6 mSv, depending on body habitus. Two patients were used to study cardiac phase variation. One was in the 36 patient cohort described above. The second was an additional patient with no CT evidence of CAD but who underwent retrospective ECG gating without tube current modulation. Twenty-five consecutive patients with ≥50% stenosis in the LAD were used to test feasibility of computing gradients from prospectively ECG gated single R-R coronary CTA (Table 1). Three of these patients were excluded because of errors in coronary segmentation; two from dense calcification and one from a coronary stent. Of the remaining 22 patients included in the study, all 7 who underwent conventional coronary angiography had confirmation of the LAD disease.

Three-hundred twenty detector-row CT images were acquired with 350 millisecond gantry rotation time and 120 kV tube voltage. Among the total 58 patients, 43 were acquired at 400 mA (standard); 15 patients were imaged at 580 mA because of a large body habitus. All patients received 80 ml iopamidol 370 mg I/ml (Isovue-370, Bracco Diagnostics, Princeton, NJ) and 40 ml saline, both at 6 ml/sec, injected with a dual injector (EZEM Empower CTA DUAL Injector, EZEM Inc, Lake Success, NY). Bolus tracking in the descending aorta was performed using a 200 HU threshold.

The target heart rate for beta-blockade (intravenous metoprolol, 5 mg increments to a maximum of 20 mg) was 65 beats per minute. There were no patients with contraindication to beta-blockade, and there were no observed or reported side effects from the beta blockers. All 58 patients received 0.4 mg sublingual nitroglycerine before imaging.

Coronary Vessel Segmentation

For each patient, at least one phase was identified to have excellent image quality for the left anterior descending (LAD), left circumflex (LCx), and right coronary artery (RCA). DICOM images from this phase were reformatted with a customized plugin for OsiriX 3.0.2 based on a 3D "virtual contrast injection" method. [7] The following data was obtained from the region of interest (ROI) defined as the entire segmented lumen at every millimeter orthogonal to the coronary center line beginning at the ostium and ending where each vessel had adequate segmentation, typically when the diameter tapered to roughly 1.5 mm: the mean and maximum attenuation (in HU), the cross-sectional area (in millimeters squared), and the shortest diameter of the cross-section or the "short axis" (in millimeters). For each vessel, a cardiovascular imager with 6 years of experience manually determined the distal point and corrected the lumen ROIs generated by the vessel segmentation software when required, for example at branch points.

Definition of Coronary Opacification Gradients

The three opacification gradients were computed using linear regression from the segmented data. The distance gradient, denoted G_d, has units of HU per centimeter of coronary artery and is defined as the slope of the regression model, measured HU = location $\times G_d + c$, where the "location" is the distance distal to ostium in centimeters, and c is a constant determined from the linear regression. Note that G_d is inherently less than zero since HU measurements decrease distally in a normal coronary artery imaged with 320-detector row CT.[6] The area gradient, denoted G_a, has units of HU per millimeter squared and is defined as the measured HU = area $\times G_a + c$ where "area" refers to the cross-sectional lumen area orthogonal to the center line. The short axis diameter gradient, denoted G_s, has units of HU per millimeter and is defined as measured HU = short axis diameter $\times G_s + c$. As with the distance gradient, the slopes and constants for the linear equations representing the cross-sectional area and short axis diameter gradients were obtained using linear regression.

Coronary opacification gradients for normal patients were computed for both the mean and maximum HU values from the vessel segmentation. Detailed analyses of contrast opacification uses the mean HU over the entire lumen. The maximum HU gradients were used for validation in normal vessels; for normal arteries the maximum HU gives an assessment relatively independent of partial volume effects.

Statistical analyses—For regression models, the Pearson correlation coefficient (r) was used to determine the strength of correlation, i.e., the goodness-of-fit. A magnitude of $r<0.25$ indicates low correlation, $0.25< r< 0.5$ moderate, $0.5< r<0.75$ strong, and $r>0.75$ excellent. We considered $p<0.05$ (two-sided t-test) to define a regression coefficient (slope) significantly different from zero.

1. General properties of gradients: The Pearson correlation coefficient and corresponding p-value were used to determine if the gradient models defined were appropriate for each normal coronary artery, i.e., if the correlation was at least moderate ($r>0.25$), and the corresponding gradient (slope) was non-zero ($p<0.05$). Only gradients meeting these criteria were further evaluated.

Gradients in patients with no CT evidence of CAD underwent one-way analysis of variances (ANOVA) to test the hypothesis that there is no significant difference of the mean gradient between the 3 major coronary arteries (LAD, LCx, and RCA).

Agreement between gradients determined from the mean versus maximum HU measurements in normal vessels was assessed using the Pearson correlation coefficient (r).

2. Variability and reproducibility of measured gradients

Heart Rate and Body Mass Index: For the 36 normal patients, linear regression models were used to determine if each of the three gradients was correlated to patient heart rate and body-mass index for each vessel. The regression coefficients were used to estimate the influence of heart rate variations between 55 and 65 beats per minute and patients with a body mass index between 20 and 30 kilograms per meter squared.

Drift Over Cardiac Phases: Linear regression models were used to evaluate for drift (i.e., a statistically significant trend) in gradient magnitude during the cardiac cycle for the LAD in the one patient who underwent retrospective ECG gating (5-95%) plus one of the 36 normal patients for whom segmentation was performed in all three arteries at all 1% intervals between 60-85%.

Inter-observer Agreement: In the patient for whom segmentation was performed at all 1% intervals between 60-85%, a second cardiovascular imager independently segmented and corrected all three arteries at 9 phases (3% intervals). Inter-observer agreement was assessed using the Pearson correlation coefficient between gradient magnitudes resulting from the individual segmentations.

3. Preliminary evaluation of gradients in patients with coronary artery disease: For the CAD cohort, all 22 patients had ≥50% LAD stenosis as determined by CT. Gradients in the LAD were computed using the same method as patients with normal coronary arteries. A two-sided *t*-test was used to assess whether each of the three gradients was the same in vessels without versus in vessels with lesions. In this case, $p < 0.05$ indicated that the mean gradient was significantly different in between the two groups of patients.

4. Phantom experiment to determine potential HU changes over the coronary artery field of view: To assess potential attenuation drift inherent to the CT scanner, HU differences were evaluated via a Delrin cylinder phantom (TOS phantom, Toshiba Medical Systems Corporation, Otawara, Japan), chosen because the properties (330 HU, density = 1.42 g/cm^3) roughly match a normal contrast enhanced coronary lumen. The phantom was scanned with one 0.5 second axial 320×0.5 mm detector row gantry rotation, 120 kV, 300 mA rotation, and 5mm reconstruction thickness. The Delrin CT number was measured via placement of a 330 mm^2 circular ROI every 5 mm over the central 13 cm of the gantry, corresponding to the location of the coronary arteries from which the three gradients are computed.

Results

1. General Properties of gradients

The cross-sectional area (G_a) and short axis diameter (G_s) opacification gradients (Figure 1) are significantly different from zero ($p=0.0001$) in all three vessels for all 36 patients with no CT evidence of CAD. Among these normal vessels, the distance gradient was not significant in the RCA for two patients and in the LAD in one patient. These were the only 3 vessels, i.e., less than 1% among a total of 324 gradients measured in 108 vessels (36 patients multiplied by 3 vessels per patient, multiplied by 3 gradients per vessel), with a Pearson $r<0.25$, indicating a non-linear association of HU and distance from the ostium. Table 2 considers the linear model fits in the remaining 105 vessels for the distance gradient and all 108 vessels for the other two models.

Regarding goodness-of-fit, the mean Pearson r values for G_s and G_a indicated excellent correlation, ranging from 0.79 (RCA) to 0.84 (LAD) and 0.77 (RCA) to 0.82 (LAD), respectively. The mean Pearson r values for G_d were slightly lower, ranging from 0.68 in the RCA to 0.80 in the LAD. Differences in significance, p, and correlation, r, between G_a and G_s were very small, likely reflecting the fact that cross-sectional area and short axis diameter are strongly related in normal coronary arteries.

Comparing the gradient between the three coronary arteries in all 36 patients (Figure 2), there was no significant difference for G_a (ANOVA $p=0.503$) and G_s (ANOVA $p=0.625$). However, the magnitude of G_d for the RCA was significantly smaller than in the LAD and LCx (ANOVA $p<0.001$).

Using the maximum HU contrast opacification gradients to evaluate the potential influence of volume averaging, less than 5% of the 324 gradients had a Pearson $r<0.25$, as opposed to <1% for the mean HU gradient definition, reflecting the fact that the maximum is not a smooth statistic. The maximum HU gradient was highly correlated to the mean HU gradient

across all patients and gradient models, indicating that volume averaging does not alter patient-specific differences in the measured gradient magnitude (Table 3, $r>0.9$ for 5 of 9 gradient models).

2. Variability and reproducibility of measured gradients

Heart Rate and Body Mass Index—Gradients exhibited significant ($p<0.05$) low to moderate (Pearson $r<0.5$) correlations with heart rate and body-mass index (Table 4). Over the range of standard coronary CTA patients, namely those with HR between 55 and 65 beats per minute and body mass index between 20 and 30 kilograms per meter squared, the correlated gradient change was less than one standard deviation of the corresponding gradient observed over the 36 patient cohort with no CAD.

Drift Over Cardiac Phases—In the single patient with reconstructions at every 1% intervals in diastole, all three gradients exhibited strong correlation with cardiac phase in the RCA and LCx (Table 5). None of the three gradients was correlated to cardiac phase in the LAD (Table 5). The LAD was further evaluated throughout the entire R-R interval for the patient with retrospective ECG-gated acquisition. For these reconstructions spaced by 5% of the R-R interval, none of the three gradients was correlated to cardiac phase in the LAD (Table 5). Example correlations in the RCA and LAD for G_a are provided in Figure 3.

The variation of the gradient magnitude through the cardiac cycle was smaller than its variation in the 36 patient cohort with no CAD (Figure 4). Gradients in the LCx demonstrated the largest variation with respect to cardiac phase.

Inter-observer Agreement—Interobserver agreement was excellent for all gradients and arteries (Table 6). In addition to high agreement, the variation in gradient magnitudes observed between readers (Table 6) was significantly smaller than both the entire sample of arteries as well as the observed cardiac phases in one patient (Figure 4).

3. Preliminary evaluation of gradients in patients with coronary artery disease

All three gradients in all 22 patients with the LAD lesions were significantly different from zero ($p=0.0001$, Figure 1). Regarding goodness-of-fit, the mean Pearson r values for G_s and G_a indicated strong correlation; for G_d there was excellent correlation (Table 2). The slight lower Pearson r values for G_s and G_d likely reflect the more challenging segmentation and subsequent imprecision in the short axis diameter and area measurements for vessels with lesions.

All three gradients in patients with LAD stenosis ≥50% had mean values significantly different ($p<0.021$) compared to the corresponding gradients in patients with no CT evidence of CAD (Figure 1). The difference was most consistent for the short axis diameter gradient (Figure 2b).

Phantom experiment to determine potential HU changes over the coronary artery field of view

The mean (range) HU measurements in the Delrin cylinder were 329.6 HU (327.8 – 332.3 HU). The very small gradient over the 4.5 HU range had a slope of 0.0225 HU/cm with the HU decreasing as measurements approached the tube anode as determined by the orientation of the phantom within the scanner.

Discussion

Wide area detector CT enables noninvasive quantitative assessment of coronary contrast changes with temporal uniformity. The current data confirms that opacification gradients exist in patients with normal coronary arteries. Customized image segmentation software is required to quantify attenuation differences over short coronary distances.

Until recently, coronary CTA was performed with retrospective ECG gating so that cardiac function could be estimated in conjunction with coronary artery disease. Because of the lower radiation dose, prospective ECG gating is used with increasing frequency; [8] with this acquisition protocol, data regarding cardiac function is not available. State-of-the-art multi-detector CT technology is now moving closer to acquiring information regarding myocardial perfusion. However, perfusion data requires specialized protocols, ideally performed at both rest and stress. Unlike the assessment of wall motion or perfusion, coronary contrast opacification gradients are simple parameters that only require post-processing tools.

We defined, computed, and analyzed three coronary contrast opacification gradients to quantify mean HU changes in normal coronary arteries. The distance gradient G_d is the linear fit that most resembles earlier work that quantifies the decrease in HU between two points in a coronary artery.[6] When compared to the cross-sectional area and short axis diameter gradients, the distance gradients may be considered easier to interpret, but in a small number of cases demonstrate nonlinearities that may limit potential clinical use. One possible reason for the slightly lower goodness-of-fit for G_d compared to G_s and G_a is the presence of branching vessels. Those linear fits inherently measure changes in HU with respect to coronary lumen size and thus are expected to be less sensitive to highly variable coronary branching patterns, a potential cause of nonlinearity in G_d. Considering only significance and correlation, the short axis diameter gradient slightly outperformed the cross-sectional area gradient. Neither of those gradients demonstrated a significant difference between the three major coronary arteries. The distance gradient was however significantly different in the RCA than in the left coronary system.

In vessels with no wall calcification, gradients computed using maximum HU values are insensitive to partial volume averaging since the voxel with maximum HU for every cross-section is expected to contain only contrast-enhanced blood. In the 108 normal vessels, the maximum HU gradients had excellent correlation with the mean HU gradients. While small wall calcium (below visual threshold for detection) could not be definitively excluded, the excellent correlation for all vessels argues that partial volume effects and imperfect segmentation do not skew gradient magnitude differences between patients.

The potential utility of gradients in coronary CTA will depend on the ease and reproducibility of the measurements as well as separation between vessels with and without CAD. Regarding gradient measurements, the required customized software can be used on current DICOM coronary CTA data. Regarding reproducibility, for the patients with no CAD, we observed limited impact of varying HR, BMI, cardiac phases, and different cardiovascular readers in comparison to variations in the patient population. In fact, many correlations such as those for HR and BMI were no more than moderate and may be irrelevant in larger populations. Regardless, the ensemble of results well-characterizes the distribution of all gradients in patients with no CAD, the primary purpose of the study.

Our understanding of gradients in diseased vessels is very sparse. However, the preliminary evaluation in 22 patients with LAD disease suggests a consistent difference with normals. Additional studies will be required to confirm the differences between patients with and without CAD for different lesion types. Initial studies will focus on patients with both focal lesions and diffuse CAD, as the latter group is expected to have differences over long

segments of the coronary arteries and have a graded, continuous pressure decrease along the length of the artery.[9]

Normal coronary arteries do not have a measurable drop in pressure along their course. However, the reproducibility of the gradient data argues that differences in opacification are linked to flow. Regarding coronary lesions, the most important factor to determine resistance is the minimum cross-sectional area,[10] incorporated into the definition of G_a.

If one or more gradients can be reliably measured across lesions or in patients with diffuse CAD, and if those gradients differ from the normal coronary gradients established in this work, these parameters could potentially be incorporated into the evaluation of CAD. It is important to acknowledge that the confirmation of clinical utility will ultimately require measures of clinical outcome from multiple centers, and thus the study of contrast opacification gradients is only in its infancy. However, the low level of HU drift for the scanner and the ease in computing the gradients makes it amenable for future work.

Limitations

All patients received sublingual nitroglycerine for coronary vasodilatation, increasing coronary blood flow. It is not possible to determine the influence on the calculated gradients, but the point could be relatively moot since essentially all coronary CTA is performed after nitroglycerine administration. All patients had identical iodinated contrast injection and bolus tracking protocols. However, the influence of contrast media volume, rate of injection, and iodine concentration will also require further evaluation. All patients were evaluated on a single CT platform that offers temporal uniformity; that is, data from the entire coronary tree was acquired at a single phase of opacification. Future work will evaluate if and how the gradients change when the image data is acquired on different CT platforms.

Another limitation is that there is no coronary catheterization confirmation that the patients presumed to have no CAD are in fact normal. This evaluation was performed retrospectively, and because of the high negative predictive value of CT, patients with a normal study typically require no additional imaging. Future work using patients with and without CAD will confirm the presence of opacification gradients in patients with no CAD confirmed with coronary catheterization. Finally, refinements in the post-processing software will advance our ability to rapidly determine the gradients with little user input. The present software requires manual correction near branch vessels. The time for a complex coronary system (all vessels) is 45 minutes (standard deviation 10 minutes). Further refinements to the software are expected to reduce the time burden to levels compatible with clinical workflow.

Conclusion

The mean HU changes along the course of a coronary artery are termed contrast opacification gradients and can be reproducibly evaluated with a 320-detector row CT acquisition. In normal coronary arteries, the gradients computed with respect to cross-sectional lumen short axis diameter and area orthogonal to the coronary center line are significant, linear, and not significantly influenced by the coronary artery (LAD vs LCx vs RCA). The moderate influence from BMI, heart rate, and cardiac phase variations are probably compatible with changes in motion artifact and signal to noise ratio currently experienced in clinical coronary CTA. Studying changes between coronary arteries in the same patient and changes within individual coronary arteries may provide insight with respect to coronary physiology not previously accessible noninvasively. Early experience in vessels with lesions demonstrates feasibility and further studies are warranted. The clinical

utility of these measurements will rely on potential differences when these new parameters are studied in patients with CAD.

References

1. Roberts WC, Jones AA. Quantitation of coronary arterial narrowing at necropsy in sudden coronary death: analysis of 31 patients and comparison with 25 control subjects. Am J Cardiol. 1979; 44:39–45. [PubMed: 88171]

2. Marcus ML, Harrison DG, White CW, McPherson DD, Wilson RF, Kerber RE. Assessing the physiologic significance of coronary obstructions in patients: importance of diffuse undetected atherosclerosis. Prog Cardiovasc Dis. 1988; 31:39–56. [PubMed: 3293119]

3. Libby P. Molecular bases of the acute coronary syndromes. Circulation. 1995; 91:2844–2850. [PubMed: 7758192]

4. Falk E, Shah PK, Fuster V. Coronary plaque disruption. Circulation. 1995; 92:657–671. [PubMed: 7634481]

5. Farb A, Tang AL, Burke AP, Sessums L, Liang Y, Virmani R. Sudden coronary death. Frequency of active coronary lesions, inactive coronary lesions, and myocardial infarction. Circulation. 1995; 92:1701–1709. [PubMed: 7671351]

6. Rybicki FJ, Otero HJ, Steigner ML, Vorobiof G, Nallamshetty L, Mitsouras D, Ersoy E, Mather RT, Judy PF, Cai T, Coyner K, Schultz K, Whitmore AG, Di Carli MF. Initial evaluation of coronary images from 320-detector row computed tomography. Int J Cardiovasc Imaging. 2008; 24:535–546. [PubMed: 18368512]

7. Wang C, Smedby Ö. Coronary artery segmentation and skeletonization based on competing fuzzy connectedness tree. Med Image Comput Assist Interv. 2007; 10(Pt 1):311–318.

8. Steigner ML, Otero HJ, Cai T, Mitsouras D, Nallamshetty L, Whitmore AG, Ersoy H, Levit NA, Di Carli MF, Rybicki FJ. Narrowing the phase window width in prospectively ECG-gated single heart beat 320-detector row coronary CT angiography. Int J Cardiovasc Imaging. 2009; 25:85–90. [PubMed: 18663599]

9. De Bruyne B, Hersbach F, Pijls NH, Bartunek J, Bech JW, Heyndrickx GR, Gould KL, Wijns W. Abnormal epicardial coronary resistance in patients with diffuse atherosclerosis but "Normal" coronary angiography. Circulation. 2001; 104:2401–2406. [PubMed: 11705815]

10. Klocke FJ. Measurements of coronary blood flow and degree of stenosis: current clinical implications and continuing uncertainties. J Am Coll Cardiol. 1983; 1:31–41. [PubMed: 6826941]
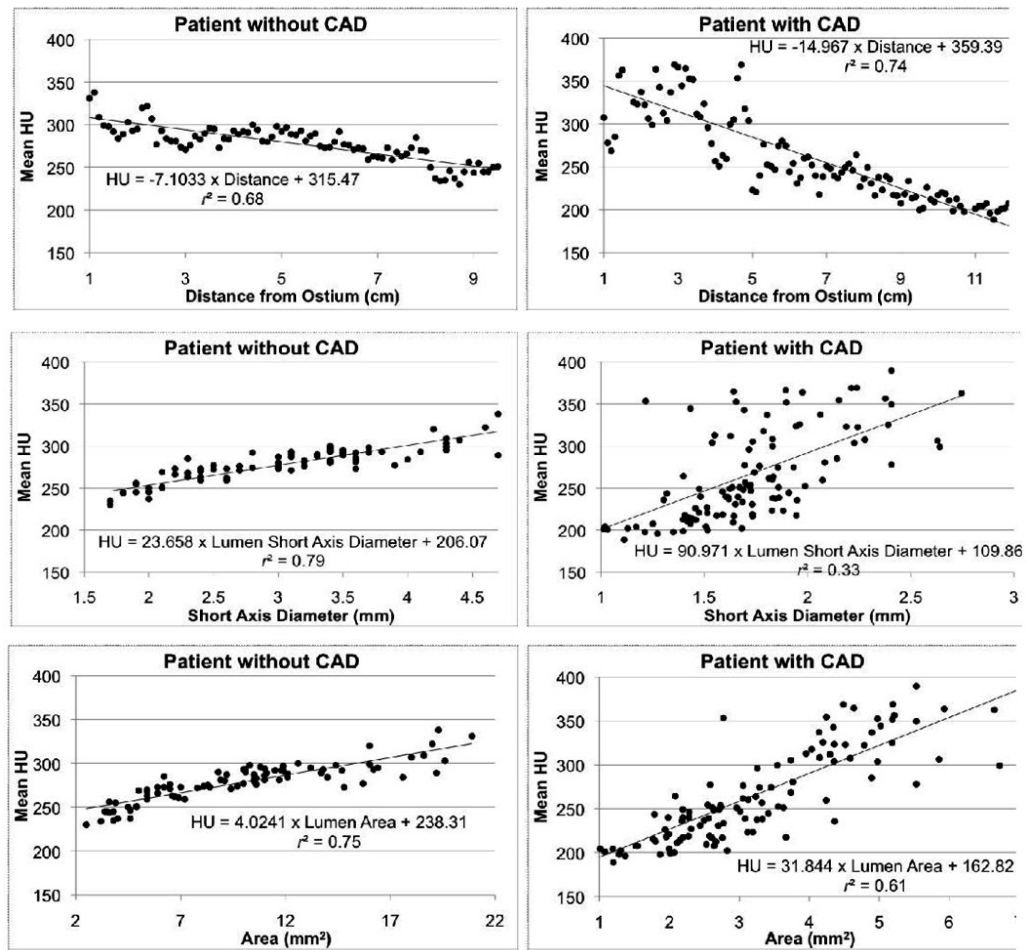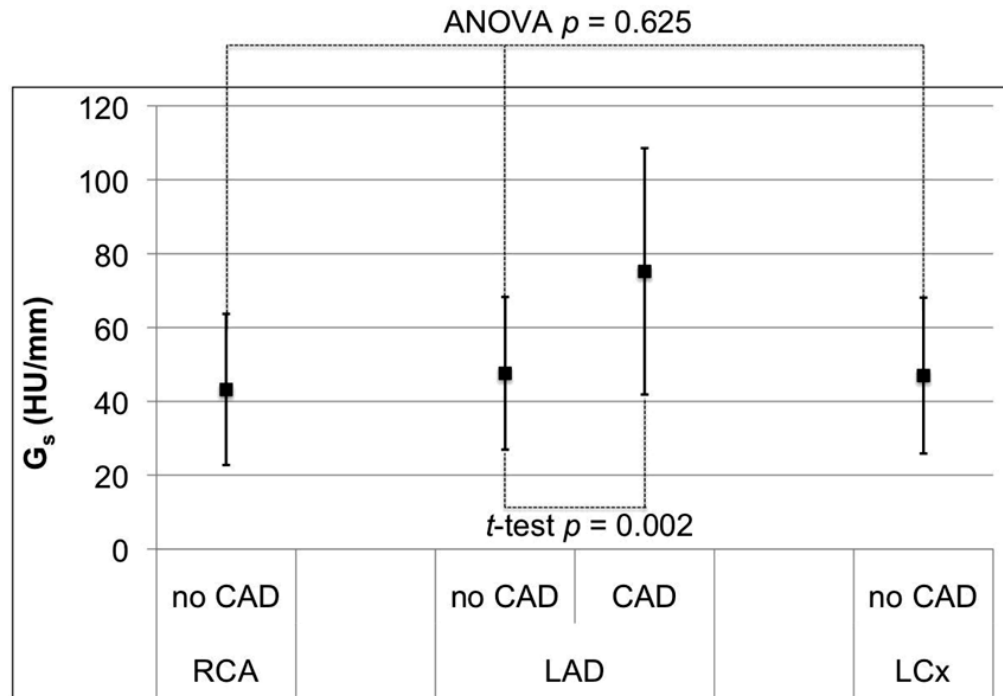
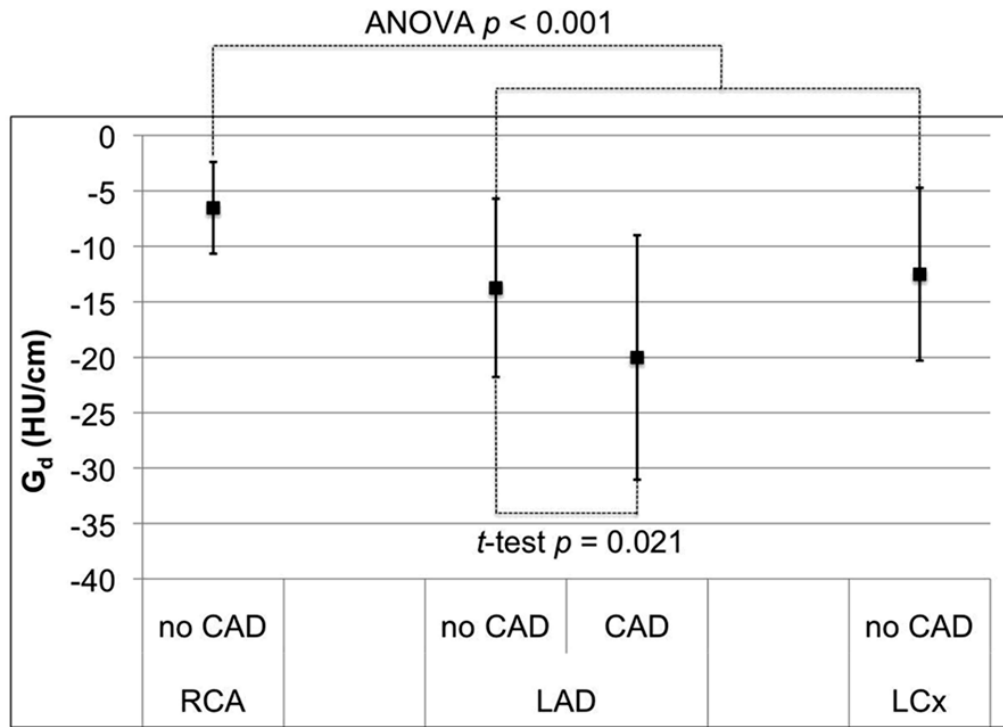**Figure 1.**
Linear fit of the distance (a), short axis diameter (b), and cross-sectional area (c) gradients in the left anterior descending (LAD) for a patient without and a patient with CT evidence of CAD, with results of linear regression.
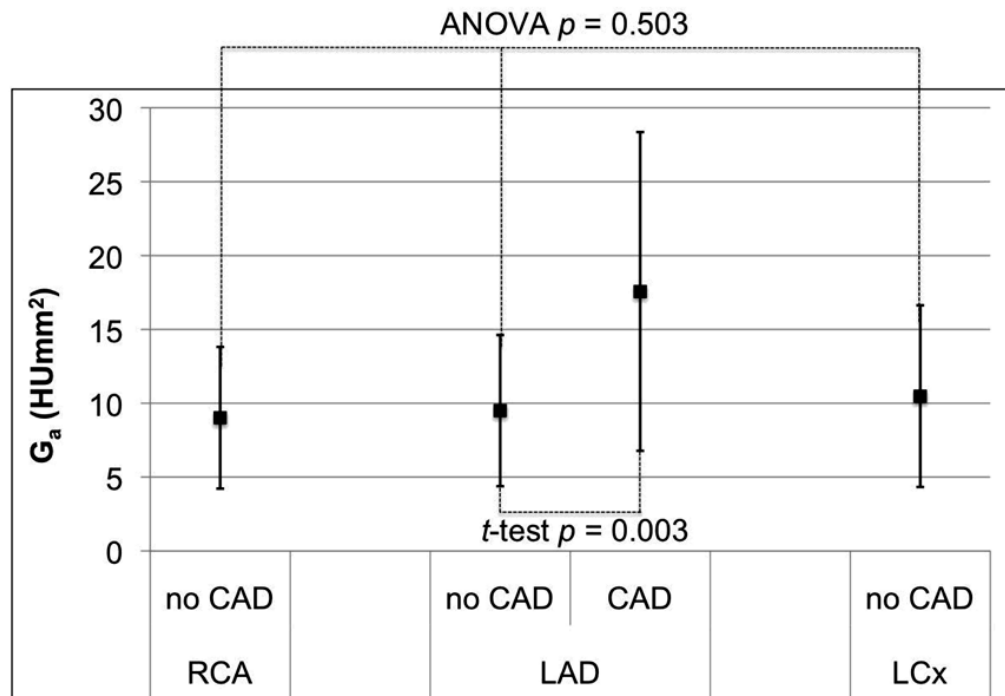
Figure 2.
Mean and standard deviation of the distance (a), short axis diameter (b), and cross-sectional area (c) gradients for the three major coronary arteries in 36 normal RCA, LAD, and LCx arteries, as well as corresponding gradients in 20 patients with LAD disease. Only the distance gradient has a significant difference between normal coronary arteries; the RCA is significantly closer to zero than the LAD and LCx (ANOVA $p < 0.001$). Patients with LAD stenosis have significantly different gradient magnitudes than normals ($p < 0.011$).
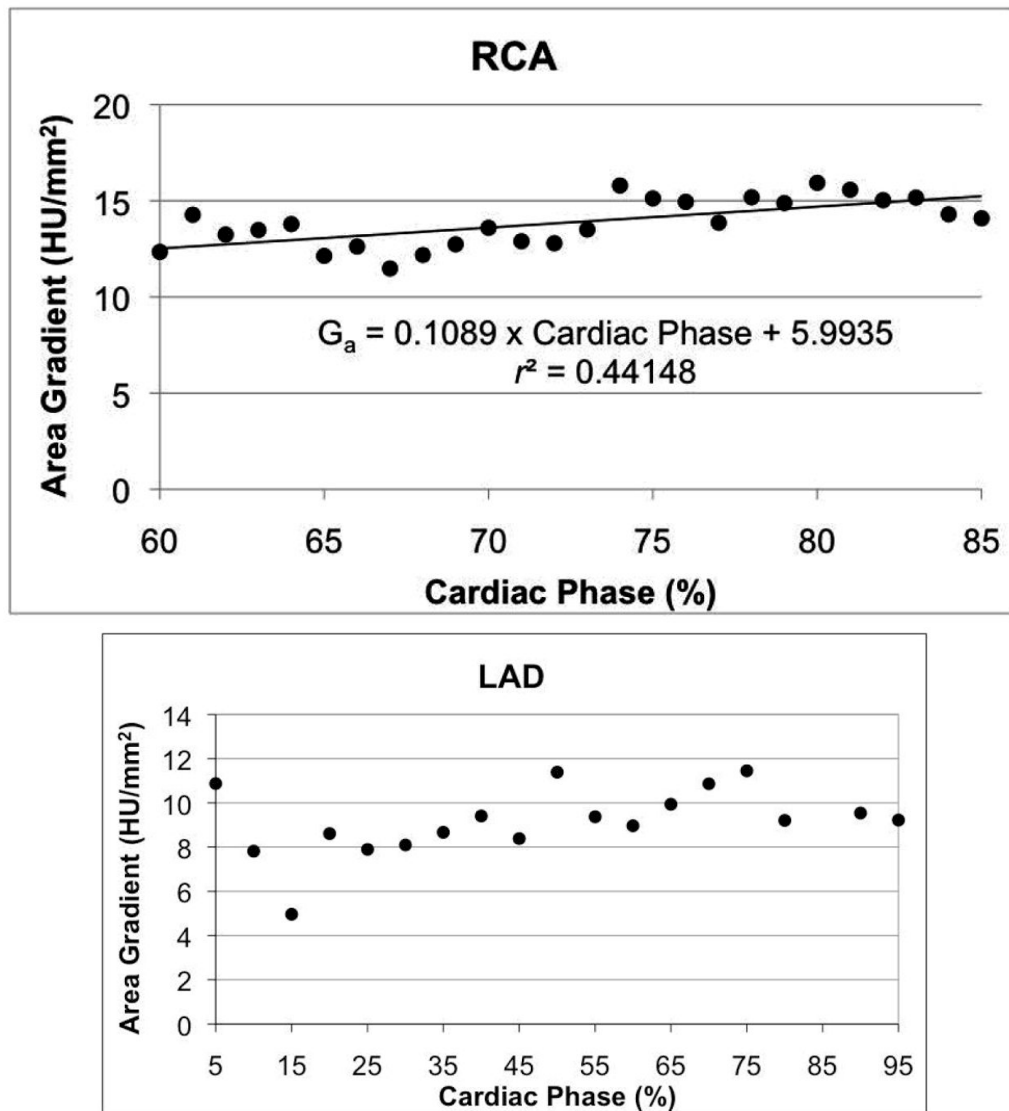
Figure 3.
Variation of area gradient with respect to cardiac phase in diastole in one RCA (a) and through the entire cardiac cycle in the LAD of a different patient (b). Linear regression results are shown for the RCA, where the trend was significant (Table 5, $p < 0.05$).

Figure 4.
Standard deviation of the magnitude for all three gradients for the 36 patients with no CT evidence of CAD (blue bars), 60-85% cardiac phase in one patient (red bars), 5-95% cardiac phase at 5% intervals in a single LAD in one patient (purple bars), and between cardiovascular imagers performing the segmentation for 9 cardiac phases in one patient (green bars).

Table 1

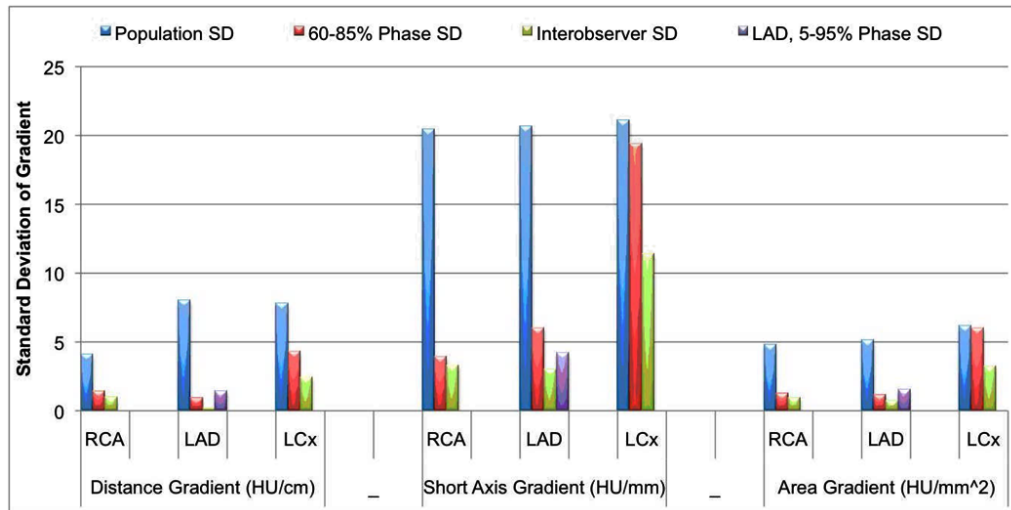Clinical indications, patient demographics, and cardiac risk factors for the 36 patients without CAD and 22 patients with CAD imaged with prospective single R-R 320-detector row CT acquisition.

		Patients without CAD	Patients with CAD	Total
	Number of patients	**36**	**22**	**58**
Indication	**Chest pain**	18	11	29
	Pre-surgical evaluation	8	1	9
	Other[*]	3	4	7
	Asymptomatic	7	6	13
Demographics	**Male**	19	16	35
	Mean age (range)	48.7 (30-66)	59.3 (35-78)	52.7 (30-78)
	BMI kg/m^2, (range)	27.8 (17.0-41.6)	27.5 (21.3-36.9)	27.7 (17.0-41.6)
	Risk Factors			
	Dyslipidemia	19	11	30
	Hypertension	13	18	31
	Obesity	10	3	13
	Diabetes	0	4	4
	Smoking	5	3	8
Beta-blockade	**None**	6	10	16
	5 mg	12	6	18
	7.5 – 10 mg	9	1	10
	>10 mg	9	5	14
Heart Rate	**mean bpm (range)**	58.2 (45-75)	58.3 (48-70)	58.3 (45-75)
	≤ 65 bpm	34	19	53
	> 65 bpm	2	3	5

[*] Other includes dyspnea and/or arm numbness/tingling

Table 2

Distance from the coronary ostium, short axis diameter, and cross-sectional area opacification gradients, with mean values, significance *p* related to a nonzero slope, and Pearson correlation coefficient *r* related to linear goodness-of-fit. Data over all 36 patients with no CT evidence of CAD is shown for the short axis diameter and cross-sectional area gradients. As noted in text, three vessels in patients with no CT evidence of CAD had a nonlinear (*r*<0.25) relationship between mean HU and distance from the ostium (2 RCA plus 1 LAD); these 3 vessels are excluded from the distance gradient computations.

	Vessel		Gradient Mean ± SD	Maximum *p*-value	Pearson *r* Mean ± SD
G_d, Distance from Ostium[1] (HU/cm)	RCA		-6.5±4.1	0.002	0.68±0.17
	LAD	No CAD	-13.7±8.0	0.026	0.80±0.15
		CAD	-20.0±11.0	<0.0001[1]	0.80±0.09
	LCx		-12.5±7.8	0.015	0.73±0.19
G_s, Short Axis Diameter (HU/mm)	RCA		43.2±20.5	<0.0001[2]	0.79±0.12
	LAD	No CAD	47.6±20.7	<0.0001[2]	0.84±0.13
		CAD	75.2±31.4	<0.0001[1]	0.68±0.14
	LCx		47.0±21.1	0.026	0.80±0.14
G_a, Area (HU/mm²)	RCA		9.0±4.8	<0.0001[2]	0.77±0.13
	LAD	No CAD	9.5±5.1	0.003	0.82±0.13
		CAD	17.6±10.8	<0.0001[1]	0.73±0.11
	LCx		10.5±6.2	0.009	0.80±0.13

[1] All 22 patients with lesions yielded p-values lower than 0.0001.

[2] All 36 patients with no CT evidence of CAD yielded p-values lower than 0.0001.

Table 3

Correlations between mean and maximum HU contrast opacification gradients in 36 patients with no CT evidence of CAD. The regression coefficient indicates the relationship between the magnitude of the contrast opacification gradient obtained from maximum HU measurements to that obtained from mean HU measurements.

Gradient	Vessel	Regression coefficient	Pearson r
Distance (G_d, HU/cm)	RCA	2.09	0.95
	LAD	2.11	0.92
	LCx	2.35	0.79
Short Axis Diameter (G_s, HU/mm)	RCA	2.16	0.89
	LAD	2.29	0.92
	LCx	2.28	0.81
Area (G_a, HU/mm^2)	RCA	2.22	0.92
	LAD	2.25	0.94
	LCx	2.85	0.89

Table 4

Correlations (*r*) and significance (*p*) between the three gradients and each artery with respect to heart rate (HR) and body-mass index (BMI) in 36 patients with no CT evidence of CAD. Significant correlations ($p<0.05$) are highlighted. The gradient change reflects the expected influence on the gradient magnitude of heart rate (55-65 bpm) and BMI (20-30 kg/m²) variations observed for coronary CTA patients, i.e., Gradient change = regression coefficient × 10 [bpm, or, kg/m²].

Correlations for Distance Gradient

	RCA		LAD		LCx	
	r	Gradient change [HU/cm]	*r*	Gradient change [HU/cm]	*r*	Gradient change [HU/cm]
HR	0.07	0.46	0.26	3.45	0.46	5.91
BMI	0.33	2.41	0.33	4.82	0.29	3.98

Correlations for Short Axis Diameter Gradient

	RCA		LAD		LCx	
	r	Gradient change [HU/mm]	*r*	Gradient change [HU/mm]	*r*	Gradient change [HU/mm]
HR	-0.22	-7.51	-0.35	-11.86	-0.40	-13.89
BMI	-0.45	-16.35	-0.45	-16.68	-0.47	-17.73

Correlations for Cross-Sectional Area Gradient

	RCA		LAD		LCx	
	r	Gradient change [HU/mm²]	*r*	Gradient change [HU/mm²]	*r*	Gradient change [HU/mm²]
HR	-0.28	-2.19	-0.41	-3.48	-0.43	-4.38
BMI	-0.39	-3.37	-0.38	-3.51	-0.37	-4.04

Table 5

Correlations of gradients with cardiac phase in all three vessels at 1% phase intervals between 60% and 85% cardiac phase in one patient, and in the LAD at 5% intervals between 5% and 95% cardiac phase in another patient. Significant trends (highlighted) are observed for all three gradients in the RCA and LCx but not the LAD.

	Gradient	Phase Range	*p*-value	Correlation Coefficient (*r*)
RCA	Distance (G_d)	60% − 85%	0.004	-0.55
	Short Axis Diameter (G_s)	60% − 85%	0.003	0.56
	Area (G_a)	60% − 85%	0.001	0.66
LAD	Distance (G_d)	60% − 85%	0.51	
		5% − 95%	0.905	
	Short Axis Diameter (G_s)	60% − 85%	0.981	
		5% − 95%	0.137	
	Area (G_a)	60% − 85%	0.630	
		5% − 95%	0.063	
LCx	Distance (G_d)	60% − 85%	0.001	0.78
	Short Axis Diameter (G_s)	60% − 85%	0.001	0.67
	Area (G_a)	60% − 85%	0.001	0.72

Table 6

Difference in gradient analyzed by two independent cardiovascular imagers (R1 and R2) for 9 diastolic cardiac phases equally spaced between 60% and 85% in one patient, and corresponding inter-observer agreement (Pearson correlation *r*).

Gradient	Vessel	R1-R2 Difference (Mean ± SD)	Pearson *r*
Distance (G_d, HU/cm)	RCA	-0.75 ± 0.97	0.93
	LAD	-0.24 ± 0.19	0.99
	LCx	0.26± 2.44	0.87
Short Axis Diameter (G_s, HU/mm)	RCA	1.72 ± 3.31	0.91
	LAD	4.26 ± 3.00	0.95
	LCx	-0.22± 11.42	0.79
Area (G_a, HU/mm^2)	RCA	0.74 ± 0.95	0.95
	LAD	1.08 ± 0.73	0.95
	LCx	0.58 ± 3.24	0.92